Potentially induced earthquakes in Oklahoma, USA: Links between wastewater injection and the 2011 M_w 5.7 earthquake sequence

Katie M. Keranen[1], Heather M. Savage[2], Geoffrey A. Abers[2], and Elizabeth S. Cochran[3]
[1]ConocoPhillips School of Geology and Geophysics, University of Oklahoma, 100 E. Boyd Street, Norman, Oklahoma 73069, USA
[2]Lamont-Doherty Earth Observatory of Columbia University, PO Box 1000, 61 Route 9W, Palisades, New York 10964, USA
[3]U.S. Geological Survey, 525 S. Wilson Avenue, Pasadena, California 91106, USA

ABSTRACT

Significant earthquakes are increasingly occurring within the continental interior of the United States, including five of moment magnitude (M_w) ≥ 5.0 in 2011 alone. Concurrently, the volume of fluid injected into the subsurface related to the production of unconventional resources continues to rise. Here we identify the largest earthquake potentially related to injection, an M_w 5.7 earthquake in November 2011 in Oklahoma. The earthquake was felt in at least 17 states and caused damage in the epicentral region. It occurred in a sequence, with 2 earthquakes of M_w 5.0 and a prolific sequence of aftershocks. We use the aftershocks to illuminate the faults that ruptured in the sequence, and show that the tip of the initial rupture plane is within ~200 m of active injection wells and within ~1 km of the surface; 30% of early aftershocks occur within the sedimentary section. Subsurface data indicate that fluid was injected into effectively sealed compartments, and we interpret that a net fluid volume increase after 18 yr of injection lowered effective stress on reservoir-bounding faults. Significantly, this case indicates that decades-long lags between the commencement of fluid injection and the onset of induced earthquakes are possible, and modifies our common criteria for fluid-induced events. The progressive rupture of three fault planes in this sequence suggests that stress changes from the initial rupture triggered the successive earthquakes, including one larger than the first.

INTRODUCTION

Three earthquakes with M_w of 5.0, 5.7, and 5.0 (moment magnitudes from Global Centroid Moment Tensor Catalog, GCMT; http://www.globalcmt.org) occurred within the North American midcontinent near Prague, Oklahoma, United States (Fig. 1) on 5, 6, and 8 November 2011 ~180 km from the nearest known Quaternary-active fault. Earthquakes with M_w ≥ 5.0 are rare in the United States east of the Rocky Mountains; however, the number per year recorded in the midcontinent increased 11-fold between 2008 and 2011, compared to 1976–2007. Of the total seismic moment released in the region, ~66% occurred in 2011 (from the GCMT). The M_w 5.7 earthquake was the largest instrumentally recorded in Oklahoma. It created shaking up to intensity VIII in the epicentral region, destroyed 14 homes, damaged many other buildings, injured 2 people, and buckled pavement (U.S. Geological Survey, 2011). In this study we refer to the M_w ≥ 5.0 earthquakes of 5, 6, and 8 November 2011 as events A, B, and C, respectively. Moment tensor solutions (from the GCMT;

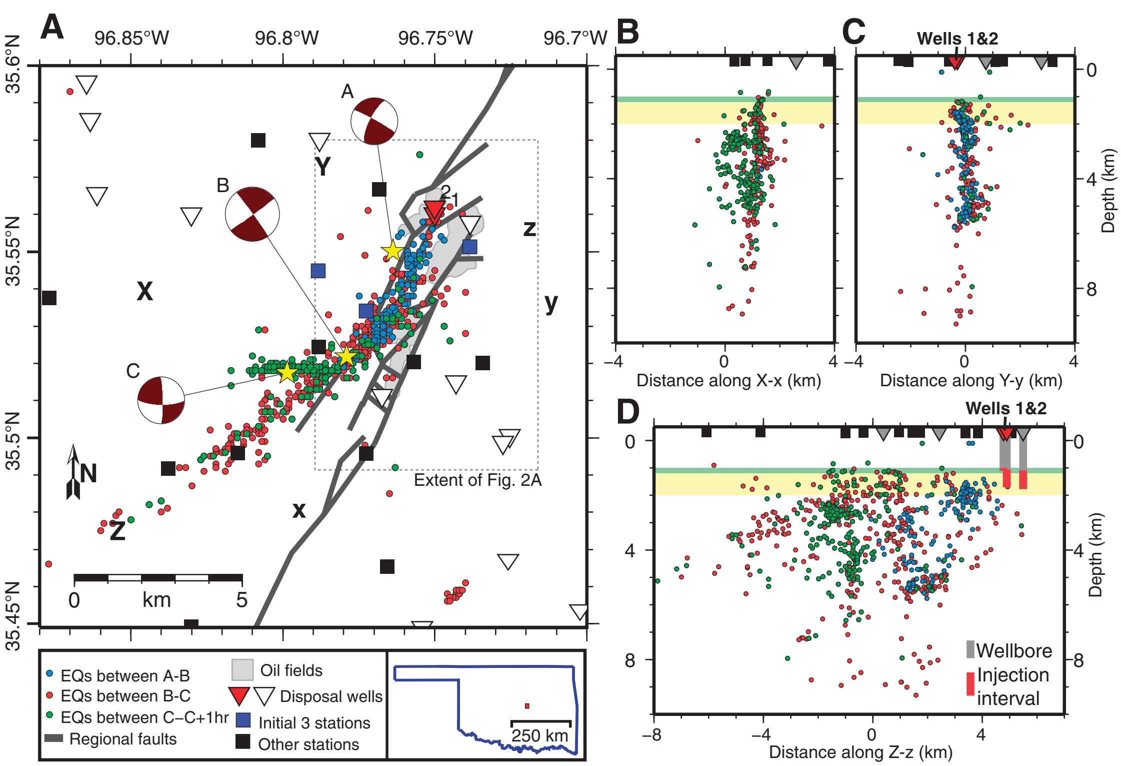

Figure 1. A: Seismicity, centroid moment tensor mechanisms, seismic stations, active disposal wells, and oil fields in central Oklahoma, United States. Epicenters of major earthquakes (EQs) are plotted at Oklahoma Geological Survey location for event A and at our relocations for events B and C, where we had sufficient control (Table DR1 [see footnote 1]). Event A likely nucleated on fault defined by aftershock locations (permitted within location error). Faults are merged from regional compilation (Joseph, 1987) and detailed local study (Way, 1983), mapped using seismic lines, well logs, and formation tops. Wells 1 and 2 inject near aftershocks of event A. B–D: Cross sections of seismicity projected from within 4 km of plane of each section. Vertical lines beneath wells indicate well path, red where perforated or open hole. Green bands denote Hunton and Simpson Groups, and yellow bands denote Arbuckle Group. Arbuckle Group overlies basement; base depth of Arbuckle Group locally is uncertain (between 1.8 and 2.2 km depth). Depths are relative to sea level, land elevation is ~300 m. Inset shows state of Oklahoma and location of map area.

GEOLOGY, June 2013; v. 41; no. 6; p. 699–702; Data Repository item 2013191 | doi:10.1130/G34045.1 | Published online 26 March 2013

Fig. 1; Table DR1 in the GSA Data Repository[1]) indicate strike-slip rupture on steeply dipping fault planes with different fault-plane orientations. Local earthquake activity began in February 2010 with an M_w 4.1 earthquake within a few kilometers of event A.

The 2010 and 2011 Prague earthquakes occurred in the structurally controlled Wilzetta oil field, within the complex, ~200-km-long, Pennsylvanian-age Wilzetta fault system (Way, 1983). Structural traps in the Wilzetta field are formed by the offset of porous limestone along high-angle faults (Fig. 2). Production of oil from the Wilzetta North field, where the earthquake sequence initiated, occurred primarily in the 1950s and 1960s from the Hunton Limestone; limited production continues. There are three active fluid injection wells located within 1.5 km of aftershocks of event A, and two within the Wilzetta North field (Fig. 1). Fluid injection in these wells began after 1993 and occurs into units from the Hunton Limestone to the deeper Arbuckle Group, predominantly dolomitic limestone, between ~1.3 and 2.1 km depth (Oklahoma Corporation Commission Well Data System: http://www.occpermit.com/WellBrowse; Fig. 2).

Earthquakes are commonly considered induced by wastewater disposal if they adhere to criteria established by Davis and Frohlich (1993) that include proximity to injection wells, a change from background seismicity, and a correlation with wastewater injection parameters. In this study we demonstrate a relationship between the 2011 Oklahoma seismicity and fluid injection, and suggest modifications to the criteria for induced earthquakes. We use the term "induced" without implying a relationship between anthropogenic stresses and earthquake magnitude, following the Committee on Induced Seismicity Potential (National Research Council of the National Academies, 2012).

METHODOLOGY

Seismic Data and Network

We deployed seismometers within 24 h of event A, and recorded the later 2 large earthquakes and thousands of aftershocks. The first 3 seismometers deployed, within 2 km of events A and B, recorded 7 h of locatable seismicity prior to event B. Additional seismometers (3) were deployed in the 24 h after event B, and 12 in the following 5 days, using digital three-component seismometers from the University of Oklahoma and the PASSCAL RAMP (Program for Array Seismic Studies of the Continental Lithosphere, Rapid Array Mobilization Program) pool. The locally recorded data were supplemented by EarthScope Transportable Array stations (Meltzer et al., 1999) at 25–150 km distance. Many stations were within 1 focal depth of the nearest earthquakes, providing accurate depth estimates; nonlinear inversions on sample hypocenters give 95% confidence bounds of <500 m in epicenter and <800 m in depth for earthquakes recorded by 3 stations before event B, and <50–100 m in epicenter and depth for those recorded by the full 18 station local array. Most ray paths were <10 km from source to station, with <2 s between S and P wave arrivals. Several hundred aftershocks per hour occurred within the first few hours of each large earthquake.

We report results based on P and S wave arrivals for (1) all identifiable events after the array installation before event B (the M_w 5.7), (2) 1–2 h time windows immediately following events B and C, and (3) larger aftershocks within 2 mo of the mainshocks and recorded on >15 stations. In most cases, both P and S wave arrival times could be picked to a precision of 10 ms or better from the local stations. Arrivals were picked manually; the high event rate caused standard automatic detection schemes to fail.

The one-dimensional velocity model (Fig. DR1 in the Data Repository) was determined by inversion methods that solve jointly for P and S wave velocities and hypocenters (Abers and Roecker, 1991) for aftershocks recorded on >15 stations. The global root mean square residual in the velocity model is 0.029 s, and influences of possible lateral variations appear to be minimal. (For details of the network, the velocity model, and location selection, see the Data Repository.)

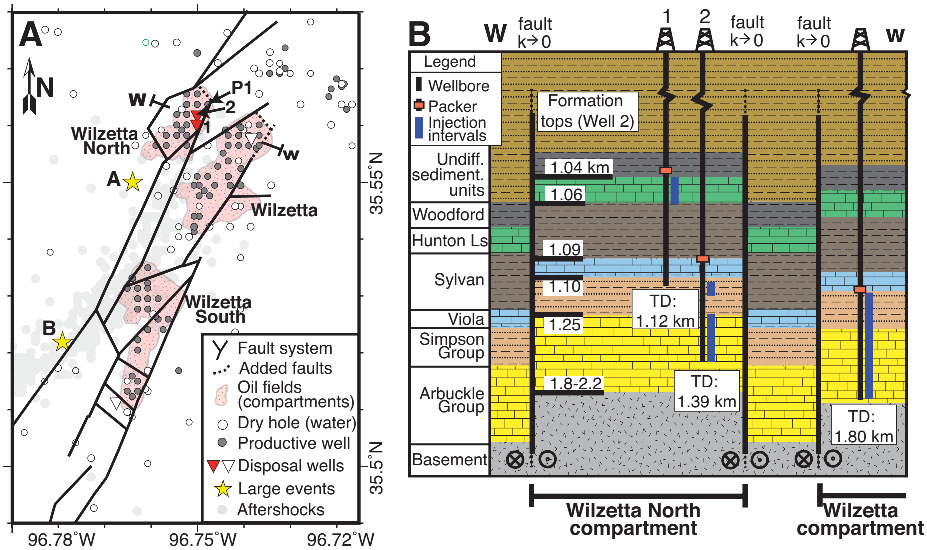

Figure 2. Subsurface geology and compartmentalization in Wilzetta oilfields, Oklahoma, United States. A: Wilzetta fault system (area shown in Fig. 1) including fault-bounded compartments, disposal wells, earthquakes, and exploration wells into Hunton Limestone or deeper units. Boundaries between producing and dry wells closely correlate to mapped faults. Wells 1, 2, and P1 are discussed in text. B: Schematic cross-section W-w across Wilzetta North and Wilzetta compartments. High-permeability reservoirs are interbedded with low-permeability shale units vertically, and faults are low-permeability barriers to fluid flow. Well paths and injection intervals are from Oklahoma Corporation Commission Well Data System (http://www.occpermit.com/WellBrowse) database. Relative offset of fault blocks is based on formation tops at closely spaced production wells (not shown). Depths to formation tops and total depth (TD) of each injection well are noted (in km below sea level).

RESULTS

Aftershock Locations and Fault Rupture Areas

For this study we located 1183 aftershocks recorded by the dense network, and show the best located 798 (see the Data Repository). We use the extent of the aftershocks measured within a few hours to days after the mainshocks to estimate the area of the faults that ruptured, as is common if an event does not rupture to the surface (e.g., Kanamori and Anderson, 1975). The aftershocks we use in this study represent <10% of the total number of earthquakes, as only a few hours of data from time periods following each $M_w \geq 5.0$ event have been examined thoroughly. Hypocenters for events A, B, and C are less well constrained than the aftershocks (see the Data Repository). However, the fault rupture sequence is clear from the focal mechanisms of the large events combined with the aftershock pattern.

The earthquakes located delineate the major seismic zones as narrow, steeply dipping planes in the sedimentary section and basement (Fig. 1), well correlated to previously identified fault structures (Way, 1983; Joseph, 1987). The strikes (from the GCMT) of events A (27°) and B

[1]GSA Data Repository item 2013191, network and event details, velocity model, and 2010–2011 injection data, is available online at www.geosociety.org/pubs/ft2013.htm, or on request from editing@geosociety.org or Documents Secretary, GSA, P.O. Box 9140, Boulder, CO 80301, USA.

(54°) parallel the two predominant orientations within the Wilzetta fault zone, and the strike of event C (91°) defines a clear secondary orientation. Therefore, three separate segments within the Wilzetta fault network ruptured successively during the sequence. The slip on the apparent fault planes of the three largest earthquakes are consistent with an east-northeast direction of maximum horizontal stress. Significantly, the northern tip of the aftershock zone for event A is in sedimentary units near an active disposal well (Fig. 1); the closest earthquakes are 200 ± 250 m distant from the wells. The depths of 83% of the aftershocks are <5 km; 30% of early aftershocks (and 20% of all earthquakes) were located within the sedimentary units into which fluids are injected (Fig. 1).

Fluid Triggering and Correlation of Seismicity to Fluid Injection Data

Earthquake triggering by fluid injection occurs if pore pressure at the fault increases beyond a critical pressure threshold (Hubbert and Rubey, 1959; Healy et al., 1968; Raleigh et al., 1976), lowering effective normal stress on a fault close to failure. In the induced seismicity experiment at Rangely, Colorado, downhole reservoir pressure measurements were available and the seismicity rate rose and fell within months of changes in reservoir pressure (Raleigh et al., 1976). Pressure data available for the Wilzetta North field are limited to monthly reported wellhead pressure (pressure at the surface while pumping), and no direct measurements of pressure within the reservoir are accessible. We thus follow standard methods and investigate possible temporal correlations between seismicity rate and surface injection parameters (e.g., Healy et al., 1968; Frohlich et al., 2011; Horton, 2012).

No short-term monthly correlation is evident in the Wilzetta field (Fig. DR2). Such a temporal correlation to surface injection parameters is rare, though evident at the Rocky Mountain Arsenal in Colorado (Healy et al., 1968). A more common observation in cases of induced seismicity is the onset of earthquakes soon after the initiation of fluid injection. Seismicity began within months of the start date of injection at the Rocky Mountain Arsenal (Healy et al., 1968), in Arkansas (Horton, 2012), and at the Dallas–Fort Worth (Texas) airport (Frohlich et al., 2011). However, within oilfields near Prague, Oklahoma, the first noted earthquake (M_w 4.1, 2010) did not occur until 17 yr after injection commenced (Fig. 3A). It is difficult to know if small earthquakes were occurring prior to 2010 near Prague, given the lack of nearby seismic stations; none were recorded or reported. A similarly long delay was observed at the Cogdell oil field in Texas (Davis and Pennington, 1989), where induced earthquakes began 20 yr after injection initiated.

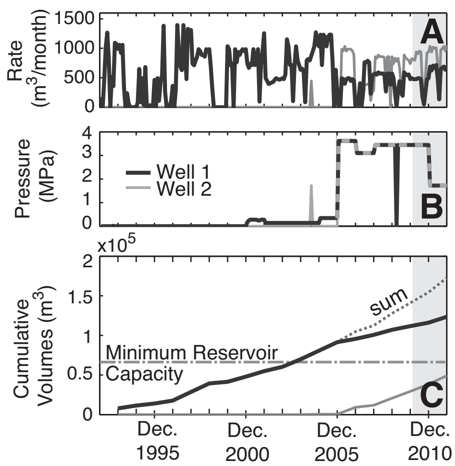

Figure 3. Available injection data. A: Monthly volumes of wastewater disposed at injection wells 1 and 2 (Fig. 2) near nucleation of event A. Monthly volumes were reported for 2002–2011; daily average volumes are multiplied by number of days per month for 1993–2002. B: Wellhead pressure for periods when pump is active, for same wells. C: Cumulative volume injected at wells 1 and 2 (from yearly totals). Minimum capacity of reservoir is denoted as horizontal dashed line and equals volume of oil extracted from Wilzetta North field, estimated by dividing total volume extracted from three Wilzetta fields by fractional area of Wilzetta North. This is absolute minimum estimate of reservoir fluid capacity; no data are available for water extracted or reinjected during production. Gray shading notes earthquakes in 2010–2011.

Increasing Injection (and Reservoir?) Pressure

Wellhead pressure in the Wilzetta North field appears fixed at a constant value during pumping, as it was at Rangely, Colorado (Gibbs et al., 1972), with multiyear intervals of constant surface pressure punctuated by step increases (Well 1; Fig. 3). Initially, fluid was injected into the Hunton Limestone in Well 1 at zero reported wellhead pressure (Oklahoma Corporation Commission Well Data System) (Fig. 3B), signifying an underpressured reservoir (below hydrostatic pressure) depleted by earlier hydrocarbon production. Wellhead pressure increased in steps, starting in 2001 at ~0.2 MPa (25–40 psi) and reaching a maximum of 3.6 MPa (525 psi) in 2006 (Fig. 3). The final tenfold increase in wellhead pressure, and the concurrent addition of a second disposal well into deeper units, came after the volume of water injected into the Hunton Limestone at Well 1 exceeded the volume of oil extracted from the Hunton strata at wells throughout the compartment (Way, 1983) (Fig. 3C). The volume of oil extracted is only an approximate estimate of reservoir capacity, and likely an underestimate; no data are available for water volume extracted or reinjected during production.

In the Wilzetta field, hydrocarbon accumulations were isolated to fault blocks of <1 km² areal extent, surrounded by water-saturated zones, indicating that the compartment-bounding faults were likely seals against fluid migration over geologic time. Such low-permeability barriers are common in sedimentary basins (Bradley and Powley, 1994) and can inhibit the diffusion of fluid pressure. In an idealized sealed reservoir, reservoir pressure gradually rises as injection volume increases (Fig. 4A), and the pressure difference between wellhead pressure (corrected for the water column) and reservoir pressure decreases (Fig. 4B), along with flow rate. When wellhead pressure is increased, as in the Wilzetta North field (Fig. 3), pressure gradient and flow rate increase. With sufficient time, volume injected, and wellhead pressure, pressure at the fault may exceed the critical pressure (Fig. 4B) and trigger slip. The time required for pressure at the fault to rise to the critical threshold in a closed compartment depends upon injection rate and reservoir volume and permeability, explaining delays before the onset of induced seismicity such as observed in this study and at the Cogdell oil field (Davis and Pennington, 1989).

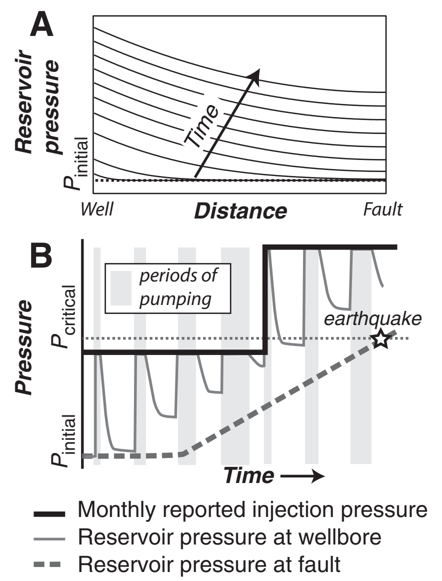

Figure 4. A: Reservoir pressure in simplistic sealed reservoir. Fluid pressure in reservoir, including at fault, rises through time as reservoir fills. Left edge of model is injection wellbore; right edge represents sealed fault. B: Predicted reservoir pressure compared to reported monthly wellhead pressure (plus weight of water column), apparently constant because pressure is reported only during pumping. Reservoir pressure near wellbore equals reported injection pressure while pumping, but drops when pump stops. Over multiple pumping cycles, time-averaged formation pressure near well rises slowly (A), and pressure gradient decreases, lowering flow rate and requiring longer periods of pumping (shaded in gray) to maintain constant monthly disposal volume. When wellhead pressure is increased, pressure gradient increases and pumping becomes more efficient.

Neither reservoir pressure data nor detailed flow rates, required to fully test this hypothesis, are available for the Prague, Oklahoma, wells. Injection rate in Oklahoma is reported as a monthly volume and the averaging of flow rate per month smooths out higher frequency variations. Alternative hypotheses to raise fluid pressure at the fault unrelated to the identified compartments, including the concurrent increase in wellhead pressure and the addition of a second injection well in 2006, cannot be rejected without reservoir pressure data. However, the agreement between original oil volume extracted and cumulative water injected prior to seismicity (Fig. 3) supports the notion that a critical volume was reached through injection in the Wilzetta North compartment.

Minor production is reported from the Hunton Limestone 500 m to the north, near the edge of the compartment (Fig. 2; well P1) (Oklahoma Corporation Commission Well Data System). It is unknown if the well is in pressure communication with the injection wells, because we have no measurements of reservoir pressure to determine connectivity. However, fluid pressure can rise throughout portions of a semirestricted reservoir following injection, and high fluid pressure can be maintained for years even if one side is infinitely open, as observed at the Rocky Mountain Arsenal (Hsieh and Bredehoeft, 1981).

DISCUSSION

Continuing injection over 18 yr into subsurface compartments in the Wilzetta field may have refilled a compartment, eventually reducing the effective stress along reservoir-bounding faults and triggering the 2010–2011 earthquakes. Injection has continued and earthquakes with magnitudes ≥3.0 continue to occur. We interpret event A (M_w 5.0) to have been induced by increased fluid pressure, exceeding the largest earthquake known to be induced by injected fluid (M_w 4.8; National Research Council of the National Academies, 2012). Aftershocks of event A appear to deepen away from the well, and may imply downward pressure propagation into basement. Event B, of much larger magnitude (M_w 5.7), and event C may also be considered consequences of injection; however, Coulomb stress calculations show that the fault geometries are consistent with triggering by stress transfer (Cochran et al., 2012). The triggering implies that the faults were close to failure, supporting the view that favorably oriented faults are critically stressed throughout the continents (Zoback et al., 2002). In this manner, small- to moderate-sized injection-induced events may result in release of additional tectonic stress. The scalar moment released in the Oklahoma sequence exceeds predictions based on the volume of injected fluid (McGarr, 1976) by several orders of magnitude, requiring the release of substantial tectonic stress.

The 2011 Prague, Oklahoma, earthquakes necessitate reconsideration of the maximum possible size of injection-induced earthquakes, and of the time scale considered diagnostic of induced seismicity. Typically, a response of seismicity to injection within months has been sought to diagnose earthquake triggering (Raleigh et al., 1976; Davis and Frohlich, 1993). Here we present a potential case of fluid injection into isolated pockets resulting in seismicity delayed by nearly 20 yr from the initiation of injection, and by 5 yr following the most substantial increase in wellhead pressure.

ACKNOWLEDGMENTS

We thank the Oklahoma Corporation Commission for the well database. The U.S. Geological Survey, the Oklahoma Geological Survey, Oklahoma State University, and the University of Oklahoma provided field support. The University of Oklahoma funded field acquisition costs. The PASSCAL (Program for Array Seismic Studies of the Continental Lithosphere) instrument center provided RAMP (Rapid Array Mobilization Program) instruments and logistical support. We thank two anonymous reviewers and M.D. Zoback, W. Ellsworth, E. Roeloffs, C. Scholz, and E. Brodsky for constructive reviews. D. Sumy, C. Hogan, G. Mattei, K. Pham, and C. Dieck picked many arrivals, helped with deployment, and/or maintained the seismic network.

REFERENCES CITED

Abers, G.A., and Roecker, S., 1991, Deep structure of an arc-continent collision: Earthquake relocation and inversion for upper mantle P and S wave velocities beneath Papua New Guinea: Journal of Geophysical Research, v. 96, p. 6379–6401, doi:10.1029/91JB00145.

Bradley, J.S., and Powley, D.E., 1994, Pressure compartments in sedimentary basins: A review, *in* Ortoleva, P.J., ed., Basin compartments and seals: American Association of Petroleum Geologists Memoir 61, p. 3–26.

Cochran, E.S., Sumy, D.F., Keranen, K.M., Abers, G.A., and Savage, H.M., 2012, Coulomb stress modeling of the 2011 M5.7 Oklahoma earthquake sequence: American Geophysical Union 2012 Fall Meeting, San Francisco, California, 3–7 December 2012, S53I–05.

Davis, S.D., and Frohlich, C., 1993, Did (or will) fluid injection cause earthquakes? Criteria for a rational assessment: Seismological Research Letters, v. 64, p. 207–224.

Davis, S.D., and Pennington, W.D., 1989, Induced seismic deformation in the Cogdell oil field of west Texas: Seismological Society of America Bulletin, v. 79, p. 1477–1495.

Frohlich, C., Hayward, C., Stump, B., and Potter, E., 2011, The Dallas–Fort Worth earthquake sequence: October 2008 through May 2009: Seismological Society of America Bulletin, v. 101, p. 327–340, doi:10.1785/0120100131.

Gibbs, J.F., Healy, J.H., Raleigh, C.B., and Coakley, J., 1972, Earthquakes in the oil field at Rangely, Colorado: U.S. Geological Survey Open File Report 72–130, 48 p., http://pubs.usgs.gov/of/1972/0130/.

Healy, J.H., Rubey, W.W., and Griggs, D.T., 1968, The Denver earthquakes: Science, v. 161, p. 1301–1310, doi:10.1126/science.161.3848.1301.

Horton, S., 2012, Disposal of hydrofracking waste fluid by injection into subsurface aquifers triggers earthquake swarm in central Arkansas with potential for damaging earthquake: Seismological Research Letters, v. 83, p. 250–260, doi:10.1785/gssrl.83.2.250.

Hsieh, P.A., and Bredehoeft, J.D., 1981, A reservoir analysis of the Denver earthquakes: A case of induced seismicity: Journal of Geophysical Research, v. 86, p. 903–920, doi:10.1029/JB086iB02p00903.

Hubbert, M.K., and Rubey, W.W., 1959, Role of fluid pressure in mechanics of overthrust faulting: Geological Society of America Bulletin, v. 70, p. 115–206, doi:10.1130/0016-7606(1959)70[115:ROFPIM]2.0.CO;2.

Joseph, L., 1987, Subsurface analysis, "Cherokee" Group (Des Monesian), portions of Lincoln, Pottawatomie, Seminole, and Okfuskee Counties, Oklahoma: The Shale Shaker, v. 12, p. 44–69.

Kanamori, H., and Anderson, D.L., 1975, Theoretical basis of some empirical relations in seismology: Seismological Society of America Bulletin, v. 65, p. 1073–1095.

McGarr, A., 1976, Seismic moments and volume changes: Journal of Geophysical Research, v. 81, p. 1487–1494, doi:10.1029/JB081i008p01487.

Meltzer, A., Rudnick, R., Zeitler, P., Levander, A., Humphreys, E., Karlstrom, K., Ekström, G., Carlson, C., Dixon, T., Gurnis, M., Shearer, P., and van der Hilst, R., 1999, The USArray Initiative: GSA Today, v. 9, no. 11, p. 8–10.

National Research Council of the National Academies (Committee on Induced Seismicity Potential in Energy Technologies, Committee on Earth Resources, Committee on Geological and Geotechnical Engineering, Committee on Seismology and Geodynamics, Board on Earth Sciences and Resources, and Division on Earth and Life Studies), 2012, Induced seismicity potential in energy technologies: Washington, D.C., National Academies Press, 300 p.

Raleigh, C.B., Healy, J.H., and Bredehoeft, J.D., 1976, An experiment in earthquake control at Rangely, Colorado: Science, v. 191, p. 1230–1237, doi:10.1126/science.191.4233.1230.

U.S. Geological Survey, 2011, Earthquake summary, magnitude 5.6 Oklahoma: http://earthquake.usgs.gov/earthquakes/recenteqsww/Quakes/usb0006klz.php.

Way, H.S.K., 1983, Structural study of the Hunton Lime of the Wilzetta Field, T12–13N, R5E, Lincoln County, Oklahoma, pertaining to the exploration for hydrocarbons [M.S. thesis]: Stillwater, Oklahoma State University, 80 p.

Zoback, M.D., Townend, J., and Grollimund, B., 2002, Steady-state failure equilibrium and deformation of intraplate lithosphere: International Geology Review, v. 44, doi:10.2747/0020-6814.44.5.383.

Manuscript received 18 September 2012
Revised manuscript received 23 January 2013
Manuscript accepted 23 January 2013

Printed in USA